ADAPTIVE NONCOHERENT LINEAR MINIMUM ISI EQUALIZATION FOR MDAPSK SIGNALS

Robert Schober, Wolfgang H. Gerstacker, and Johannes B. Huber

Laboratorium für Nachrichtentechnik, Universität Erlangen–Nürnberg
Cauerstraße 7, D–91058 Erlangen, Germany
e-mail: {*schober, gersta, huber*}*@LNT.de*, WWW: *http://www.LNT.de/~dcg*

Abstract — **In this paper, a novel noncoherent linear equalization scheme is introduced and analyzed. The proposed scheme is not only applicable for M–ary differential phase–shift keying (MDPSK) but also for M–ary differential amplitude/phase–shift keying (MDAPSK) and minimizes the variance of intersymbol interference (ISI) in the equalizer output signal. The optimum equalizer coefficients may be calculated directly from an eigenvalue problem. For an efficient recursive adaptation of the equalizer coefficients, a modified least–mean–square (LMS) algorithm is proposed. Simulations confirm the good performance of the considered noncoherent equalization scheme and its robustness against frequency offset.**

1. Introduction

The combination of linear or nonlinear equalization and coherent detection (CD) has been studied extensively in literature (see e.g. [1, 2] and references therein) and is applied in many existing communication systems. However, only few results are available for *noncoherent* equalization schemes, i.e., for the combination of linear or nonlinear equalization and noncoherent detection. Such noncoherent receivers have the important advantage of being more robust against phase noise and frequency offset than coherent equalization schemes.

Noncoherent linear minimum mean–squared error (MMSE) equalization has been proposed in [3, 4], while noncoherent decision–feedback equalization (DFE) has been regarded in [5, 6]. These noncoherent equalizers have in common that they are only designed for MDPSK, which may be considered as a special case of MDAPSK. However, recently MDAPSK constellations with more than one amplitude level have become very popular because of their high spectral efficiency (see e.g. [7, 8] and references therein). Therefore, it is desirable to derive robust noncoherent linear equalization (NLE) schemes for general MDAPSK signals. A noncoherent MMSE equalizer for 16DAPSK has been considered in [9], however, it turned out that a theoretical analysis of this equalizer is very difficult if not impossible.

Similar to the schemes given in [4, 9], the proposed NLE scheme consists of a linear equalizer combined with a decision–feedback differential detector (DF–DD) [7, 8]. In contrast to the NLE schemes considered in [4, 9], the NLE scheme proposed here minimizes the variance of intersymbol interference (ISI) in the equalizer output signal and thus, will be referred to as noncoherent minimum ISI equalization (NMIE). The essential difference to all previously proposed noncoherent equalization schemes [3, 4, 5, 6, 9] is that a closed–form solution for the equalizer coefficients exists. If an infinite–length filter is employed, a zero–forcing (ZF) equalizer results.

For adaptation of the equalizer coefficients a modified least–mean–square (LMS) algorithm is presented. Simulations confirm the high performance of the proposed scheme and its robustness against frequency offset.

2. Transmission Model and Receiver Structure

Fig. 1 shows a block diagram of the discrete–time transmission model. All signals are represented by their complex baseband equivalents. For simplicity, only T–spaced equalizers are considered here. The transmitted MAPSK symbols $s[k]$ are given by $s[k] \triangleq R[k]b[k]$, $k \in \mathbb{Z}$, with absolute amplitude symbol $R[k]$, $R[k] \in \{R_1, \ldots, R_Z\}$ ($Z = 1$, i.e., $R[k] \equiv 1, \forall k$, for MPSK) and absolute phase symbol $b[k] \in \{e^{j2\pi\nu/(M/Z)} | \nu \in \{0, 1, \ldots, M/Z - 1\}\}$. For convenience, $\mathcal{E}\{|s[k]|^2\}$ ($\mathcal{E}\{\cdot\}$ denotes expectation) is normalized to unity. $s[k]$ is obtained from the MDAPSK symbol

$$\Delta s[k] \triangleq \Delta R[k]a[k] \tag{1}$$

via differential encoding:

$$s[k] = \Delta s[k]s[k-1]. \tag{2}$$

$\Delta R[k] = R[k]/R[k-1]$ ($\Delta R[k] \equiv 1, \forall k$, for MDPSK) and $a[k] = b[k]/b[k-1]$, denote the amplitude and the phase difference symbol, respectively. The most popular MDAPSK signaling format is 16DAPSK (16–star QAM) and will be used for the simulations presented in Section

This work was supported by TCMC (Technology Centre for Mobile Communication), Philips Semiconductors, Germany.

5. Here, $Z = 2$ is valid, i.e., there are two different amplitude levels R_1 and R_2, $R_1 < R_2$, and the amplitude ratio is given by $\Delta R = R_2/R_1$. One information bit is mapped to the amplitude difference symbol, while three information bits are Gray–mapped to the phase difference symbol. $\Delta R[k] = 1$ and $\Delta R[k] = \Delta R$ (if $R[k-1] = R_1$) or $\Delta R[k] = 1/\Delta R$ (if $R[k-1] = R_2$) is valid if the corresponding information bit is equal to zero and one, respectively.

The MAPSK symbols $s[k]$ are transmitted over an ISI producing channel with unknown, constant phase shift Θ. The discrete–time received signal, sampled at times kT at the output of the receiver input filter, can be expressed as

$$r[k] = \mathrm{e}^{j\Theta} \sum_{\nu=0}^{L_h-1} h_\nu s[k-\nu] + n[k], \tag{3}$$

where h_ν, $0 \le \nu \le L_h - 1$, are the coefficients of the combined discrete–time impulse response of the cascade of transmit filter, channel, and receiver input filter; its length is denoted by L_h. For the receiver input filter, we assume a square–root Nyquist frequency response. Thus, the zero mean complex Gaussian noise $n[\cdot]$ is white. Due to an appropriate normalization, the noise variance is $\sigma_n^2 = \mathcal{E}\{|n[k]|^2\} = N_0/E_S$. E_S and N_0 are the mean received energy per symbol and the single–sided power spectral density of the underlying passband noise process, respectively. The equalizer output symbol $q[k]$ may be written as

$$\begin{aligned} q[k] &= \sum_{\nu=0}^{L_c-1} c_\nu r[k-\nu] \\ &= \mathrm{e}^{j\Theta} g_{k_0} s[k-k_0] + \mathrm{e}^{j\Theta} \sum_{\substack{\nu=0 \\ \nu\neq k_0}}^{L_h+L_c-2} g_\nu s[k-\nu] \\ &\quad + \sum_{\nu=0}^{L_c-1} c_\nu n[k-\nu], \end{aligned} \tag{4}$$

where c_ν are the equalizer coefficients and

$$g_\nu = \sum_{\mu=0}^{L_c-1} c_\mu h_{\nu-\mu} \tag{5}$$

are the coefficients of the combined impulse response of overall channel and equalizer; L_c is the equalizer length. The decision delay k_0 should be optimized since it can affect performance significantly.

The next stage of the proposed receiver is a DF–DD [7, 8], which determines an estimate $\Delta\hat{s}[k-k_0]$ for the transmitted symbol $\Delta s[k-k_0]$ based on a reference symbol

$$q_{\mathrm{ref}}[k-1] = \frac{\sum_{\nu=1}^{N-1} q[k-\nu] \prod_{\mu=1}^{\nu-1} \frac{1}{\Delta\hat{s}^*[k-k_0-\mu]}}{\sum_{\nu=1}^{N-1} \prod_{\mu=1}^{\nu-1} \frac{1}{|\Delta\hat{s}[k-k_0-\mu]|^2}}, \tag{6}$$

where N, $N \ge 2$, is the number of equalizer output symbols used for determination of $\Delta\hat{s}[k-k_0]$ (cf. (7)).

The decision variable for estimation of $\Delta\hat{s}[k-k_0]$ is given by

$$d[k] = \frac{q[k]}{q_{\mathrm{ref}}[k-1]}. \tag{7}$$

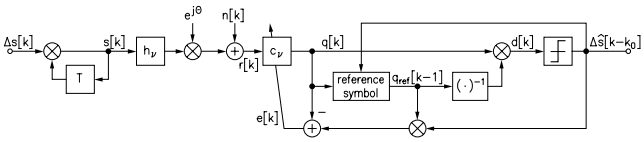

Figure 1: Block diagram of the discrete–time transmission model with NMIE.

3. Noncoherent Minimum ISI Equalization

3.1. Noncoherent Cost Function

First, the cost function for NMIE is derived. As usual, it is assumed that all decision–feedback symbols $\Delta\hat{s}[\cdot]$ are correct, i.e, $\Delta\hat{s}[k-k_0-\nu] = \Delta s[k-k_0-\nu]$, $\nu \ge 0$. Hence, the reference symbol according to (6) can be rewritten to

$$q_{\mathrm{ref}}[k-1] = s[k-k_0-1] \frac{\sum_{\nu=1}^{N-1} q[k-\nu] s^*[k-k_0-\nu]}{\sum_{\nu=1}^{N-1} |s[k-k_0-\nu]|^2}, \tag{8}$$

where (2) has been used.

NMIE minimizes the variance of the error signal

$$e[k] = \Delta s[k-k_0] q_{\mathrm{ref}}[k-1] - q[k], \tag{9}$$

cf. Fig. 1. Note that in the absence of noise and ISI $e[k] = 0$, $\forall\, k$, for $c_{k_0} = 1$ and $c_\nu = 0$, $\nu \ne k_0$. Taking into account the uncorrelatedness of $s[\cdot]$ and $n[\cdot]$, and the symmetry of the employed signal constellation, the variance $\sigma_e^2(\boldsymbol{c})$ ($\boldsymbol{c} \triangleq [c_0\ c_1\ \ldots\ c_{L_c-1}]^H$, $[\cdot]^H$ denotes Hermitian transposition) of the error signal $e[k]$ can be calculated to [10]

$$\sigma_e^2(\boldsymbol{c}) = \mathcal{E}\{|e[k]|^2\} = \sum_{\substack{\mu=0 \\ \mu\neq k_0}}^{L_h+L_c-2} x_\mu |g_\mu|^2 + \gamma\sigma_n^2 \sum_{\mu=0}^{L_c-1} |c_\mu|^2, \tag{10}$$

where the definitions

$$x_\mu \triangleq 1 + \mathcal{E}\left\{ |s[k-k_0]|^2 \cdot \frac{\sum_{\nu=1}^{N-1} |s[k-\mu-\nu]|^2 |s[k-k_0-\nu]|^2}{\left(\sum_{\nu=1}^{N-1} |s[k-k_0-\nu]|^2\right)^2} \right\} \quad (11)$$

and

$$\gamma \triangleq 1 + \mathcal{E}\left\{ \frac{1}{\sum_{\nu=1}^{N-1} |s[k-k_0-\nu]|^2} \right\} \quad (12)$$

are used. In the Appendix, it is shown that, in some special cases, the expressions for x_μ and γ can be simplified considerably.

In the following, the definition

$$\boldsymbol{h}_\mu \triangleq [h_\mu \; h_{\mu-1} \; \ldots \; h_{\mu-L_c+1}]^T \quad (13)$$

($[\cdot]^T$ denotes transposition) is used. Note that $h_\mu = 0$ is valid for $\mu < 0$ and $\mu > L_h - 1$.

Using this and (5), (10) can be rewritten to

$$\begin{aligned}\sigma_e^2(\boldsymbol{c}) &= \boldsymbol{c}^H \left(\sum_{\substack{\mu=0 \\ \mu \neq k_0}}^{L_h+L_c-2} x_\mu \boldsymbol{h}_\mu \boldsymbol{h}_\mu^H \right) \boldsymbol{c} + \gamma\sigma_n^2 \boldsymbol{c}^H \boldsymbol{c} \\ &= \boldsymbol{c}^H \boldsymbol{H} \boldsymbol{c} + \gamma\sigma_n^2 \boldsymbol{c}^H \boldsymbol{c}, \end{aligned} \quad (14)$$

where the positive semi–definite Hermitian matrix $\boldsymbol{H}$ is defined as

$$\boldsymbol{H} \triangleq \sum_{\substack{\mu=0 \\ \mu \neq k_0}}^{L_h+L_c-2} x_\mu \boldsymbol{h}_\mu \boldsymbol{h}_\mu^H. \quad (15)$$

NMIE should minimize the error variance $\sigma_e^2(\boldsymbol{c})$, however, an unconstrained minimization of $\sigma_e^2(\boldsymbol{c})$ yields the all zero vector with L_c rows $\boldsymbol{c} = \boldsymbol{0}_{L_c}$. Therefore, a constraint has to be introduced. Here, the unit–energy constraint for the equalizer coefficients is employed:

$$\boldsymbol{c}^H \boldsymbol{c} = 1. \quad (16)$$

For minimization of (14) under the constraint (16), the Lagrange cost function

$$J_L(\boldsymbol{c}) \triangleq \boldsymbol{c}^H \boldsymbol{H} \boldsymbol{c} + \gamma\sigma_n^2 \boldsymbol{c}^H \boldsymbol{c} + \eta(1 - \boldsymbol{c}^H \boldsymbol{c}) \quad (17)$$

can be defined, where η is the Lagrange multiplier.

The cost function $J_L(\boldsymbol{c})$ of (17) does not depend on the channel phase Θ. Hence, it may be considered as a *non-coherent* cost function.

3.2. Stationary Points of the Cost Function

The stationary points of the cost function can be obtained by using the method for complex differentiation described in Appendix B of [11]:

$$\frac{\partial J_L(\boldsymbol{c})}{\partial \boldsymbol{c}^*} = \boldsymbol{H}\boldsymbol{c} + (\gamma\sigma_n^2 - \eta)\,\boldsymbol{c}, \quad (18)$$

and setting the result equal to zero. This yields the eigenvalue problem

$$\boldsymbol{H}\boldsymbol{c} = (\eta - \gamma\sigma_n^2)\,\boldsymbol{c} \triangleq \lambda\,\boldsymbol{c}, \quad (19)$$

where λ denotes the eigenvalue. Since $\boldsymbol{H}$ is a Hermitian positive semi–definite matrix, there are L_c vectors $\boldsymbol{c}_\nu$, $0 \leq \nu \leq L_c - 1$, of unit length[1], which solve (19), corresponding to L_c real, non–negative eigenvalues λ_ν, $0 \leq \nu \leq L_c - 1$ [11]. In [10], it is shown that the eigenvector $\boldsymbol{c}_{\text{opt}}$ corresponding to the minimum eigenvalue $\lambda_{\min}$ minimizes the cost function $J_L(\boldsymbol{c})$ and the error variance $\sigma_e^2(\boldsymbol{c})$, whereas the eigenvector corresponding to the maximum eigenvalue maximizes $J_L(\boldsymbol{c})$ and $\sigma_e^2(\boldsymbol{c})$. The remaining eigenvectors correspond to saddle points.

The minimum error variance is given by

$$\sigma_e^2(\boldsymbol{c}_{\text{opt}}) = J_L(\boldsymbol{c}_{\text{opt}}) = \lambda_{\min} + \gamma\sigma_n^2. \quad (20)$$

(19) shows that the noise variance σ_n^2 has no influence on the optimum equalizer coefficients $\boldsymbol{c}_{\text{opt}}$; it only influences the minimum error variance (cf. (20)). This implies that the resulting equalizer is related to a ZF equalizer. However, in contrast to ZF equalization, in general, NMIE forces the coefficients g_ν, $\nu \neq k_0$, of the overall impulse response not to zero, but it minimizes them in the mean–square sense (cf. (10), (17)).

3.3. Infinite–Length Equalizer

The error variance corresponding to $\boldsymbol{c}_{\text{opt}}$ becomes minimum for $\lambda_{\min} = 0$, i.e., if $\boldsymbol{H}$ is a singular matrix. In this case

$$\sigma_e^2(\boldsymbol{c}_{\text{opt}}) = J_L(\boldsymbol{c}_{\text{opt}}) = \gamma\sigma_n^2 \quad (21)$$

results from (20). From (10), it can be seen that (21) is obtained, if and only if $g_\mu = 0$, $\mu \neq k_0$. This corresponds to a transfer function of the resulting equalizer given by

$$C(\mathrm{e}^{j2\pi fT}) = \frac{\mathrm{e}^{-j2\pi fTk_0}\,p}{H(\mathrm{e}^{j2\pi fT})}, \quad (22)$$

where $H(\mathrm{e}^{j2\pi fT})$ and p denote the transfer function[2] of the discrete–time channel and a complex constant, respectively. Up to the constant p, infinite–tap NMIE is identical with coherent ZF equalization [1, 2].

[1] Note, that $\boldsymbol{c}_\nu$ is only unique up to a complex factor of magnitude one.

[2] We assume that $H(\mathrm{e}^{j2\pi fT})$ has no spectral nulls.

From (16),

$$T \int_{-1/(2T)}^{1/(2T)} |C(\mathrm{e}^{j2\pi fT})|^2 \mathrm{d}f = 1 \tag{23}$$

follows. Using this and (22), $|p|$ can be calculated to

$$|p| = \frac{1}{\sqrt{T \int_{-1/(2T)}^{1/(2T)} \frac{1}{|H(\mathrm{e}^{j2\pi fT})|^2} \mathrm{d}f}}. \tag{24}$$

Note, that the phase of p is arbitrary. The transfer function $G(\mathrm{e}^{j2\pi fT})$ of the combination of equalizer and overall channel is given by

$$G(\mathrm{e}^{j2\pi fT}) = H(\mathrm{e}^{j2\pi fT}) C(\mathrm{e}^{j2\pi fT}) = \mathrm{e}^{-j2\pi fTk_0}\, p. \tag{25}$$

Since $G(\mathrm{e}^{j2\pi fT})$ is the Fourier transform of g_k,

$$g_{k_0} = p \tag{26}$$

follows.

3.4. Performance for $N \to \infty$

In the following, we derive the limiting performance of the infinite–length equalizer for $N \to \infty$. In this case,

$$q_{\mathrm{ref}}[k-1] = \mathrm{e}^{j\Theta} g_{k_0} s[k-k_0-1] \tag{27}$$

holds in the mean–square sense [10] and the decision variable of the infinite–length equalizer is

$$d[k] = \frac{s[k-k_0]}{s[k-k_0-1]} + \frac{\sum_{\nu=0}^{L_c-1} c_\nu n[k-\nu]}{\mathrm{e}^{j\Theta} g_{k_0} s[k-k_0-1]}. \tag{28}$$

From (28) it can be seen that the signal–to–noise ratio (SNR) of NMIE can be expressed as

$$\begin{aligned} \mathrm{SNR} &= \frac{\mathcal{E}\left\{ \left| \frac{s[k-k_0]}{s[k-k_0-1]} \right|^2 \right\}}{\mathcal{E}\left\{ \left| \frac{\sum_{\nu=0}^{L_c-1} c_\nu n[k-\nu]}{g_{k_0} s[k-k_0-1]} \right|^2 \right\}} \\ &= \frac{|g_{k_0}|^2}{\sigma_n^2}, \end{aligned} \tag{29}$$

where (16) is used. Applying (24) and (26) in (29) yields

$$\mathrm{SNR} = \frac{1}{\sigma_n^2\, T \int_{-1/(2T)}^{1/(2T)} \frac{1}{|H(\mathrm{e}^{j2\pi fT})|^2} \mathrm{d}f}. \tag{30}$$

The same expression can be obtained for a coherent infinite–length ZF equalizer for MAPSK, i.e., if no differential encoding is employed [2]. Note that we assumed for our analysis $\Delta\hat{s}[k-k_0-\nu] = \Delta s[k-k_0-\nu]$, $\nu > 0$, i.e., all feedback symbols are correct. This explains, why the resulting equalizer (which is not implementable, of course) is lower–bounded by a coherent infinite–length ZF equalizer for MAPSK. The simulations in Section 5 show that realizable NMIE (i.e., without genie) is lower–bounded by coherent infinite–length ZF equalization for M**D**APSK.

4. LMS Algorithm

4.1. Derivation

A gradient algorithm is given by

$$\hat{\boldsymbol{c}}[k+1] = \boldsymbol{c}[k] - \delta_{\mathrm{LMS}} \frac{\partial}{\partial \boldsymbol{c}^*[k]} |e[k]|^2 \tag{31}$$

and

$$\boldsymbol{c}[k+1] = \frac{\hat{\boldsymbol{c}}[k+1]}{||\hat{\boldsymbol{c}}[k+1]||_2}, \tag{32}$$

where δ_{LMS} is the adaptation step size parameter ($||\cdot||_2$ denotes the L_2–norm of a vector). $\boldsymbol{c}[k] \triangleq [c_0[k]\ c_1[k]\ \ldots\ c_{L_c-1}[k]]^H$ is the equalizer coefficient vector which is now time–variant. (32) ensures that the constraint given by (16) is fulfilled. $e[k]$ is given by

$$e[k] = \Delta\hat{s}[k-k_0] q_{\mathrm{ref}}[k-1] - \boldsymbol{c}^H[k] \boldsymbol{r}[k], \tag{33}$$

with

$$\boldsymbol{r}[k] = [r[k]\ r[k-1]\ \ldots\ r[k-L_c+1]]^T. \tag{34}$$

Note that $q_{\mathrm{ref}}[k-1]$ depends only on $\boldsymbol{c}[k-\nu]$, $\nu > 0$, but not on $\boldsymbol{c}[k]$. Therefore, it has to be treated like a constant for differentiation with respect to $\boldsymbol{c}[k]$ (cf. [3, 5]). Hence, (31) may be rewritten to

$$\hat{\boldsymbol{c}}[k+1] = \boldsymbol{c}[k] + \delta_{\mathrm{LMS}} e^*[k] \boldsymbol{r}[k]. \tag{35}$$

The resulting modified LMS algorithm consists of (32), (33), and (35). It is shown in [10] that the modified LMS algorithm enjoys global convergence and minimizes the noncoherent cost function (17) for all practical relevant cases.

4.2. Convergence Speed of the Modified LMS Algorithm

Fig. 2 shows learning curves $J'[k]$ for the proposed modified LMS algorithm ($\delta_{\mathrm{LMS}} = 0.01$) for a QDPSK constellation ($M = 4$). The impulse response of the channel adopted from [2] is $h_0 = 0.304$, $h_1 = 0.903$, $h_2 = 0.304$ ($L_h = 3$), and $10\log_{10}(E_b/N_0) = 10$ dB ($E_b = E_S/\log_2(M) = E_S/2$ is the mean received energy per bit) is valid. The equalizer length is chosen to $L_c = 7$ and the decision delay is $k_0 = 4$. In order to demonstrate that the convergence speed of the proposed algorithm is similar to

that of the conventional LMS algorithm, we also included the learning curves for a conventional LMS ($\delta_{\mathrm{LMS}} = 0.01$) [2, 11]. However, it has to be mentioned that the error signals of modified and conventional algorithm are completely different. Therefore, a direct comparison of the steady–state error is **not** possible. For the modified LMS algorithm, $J'[k] = \mathcal{E}\{|e[k]|^2\}$ is valid, whereas for the conventional LMS algorithm, the definition proposed in [11] is used. In all cases, averaging is done over 1000 adaptation processes; $\boldsymbol{c}[0]$ is initialized with $c_{k_0}[0] = 1.0$, $c_\mu[0] = 0$, $\mu \neq k_0$, and a training sequence is used. It can be seen from Fig. 2 that the steady–state error of the modified LMS algorithm decreases as N increases. The dashed lines correspond to the theoretical steady–state error variance of infinite–length NMIE calculated from (21) and (39). There is a good agreement between theory and simulation. The simulated steady–state error is slightly higher since a finite–length equalizer is used and because of gradient noise. It can be seen that the convergence speed of the modified LMS algorithm is hardly influenced by N and is similar to that of the conventional LMS algorithm.

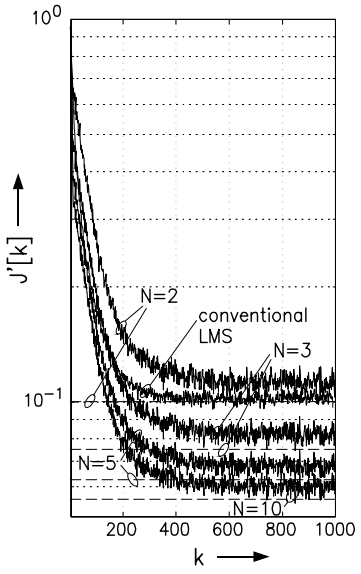

Figure 2: Learning curves for modified and conventional LMS algorithm (QDPSK constellation).

5. Simulation Results

In this section, the performance of the proposed NMIE scheme is evaluated for QDPSK and 16DAPSK by computer simulations. The equalizer coefficients are adapted by the modified LMS algorithm ($\delta_{\mathrm{LMS}} = 0.001$). A training sequence is transmitted until steady state is reached; then the equalizer operates in the decision–directed mode.

For 16DAPSK, the novel NMIE scheme is compared with coherent ZF equalization [2]. The coherent scheme determines an estimate $\hat{s}[k - k_0]$ for the transmitted MAPSK symbol $s[k - k_0]$, and subsequently differential encoding is inverted ($\Delta\hat{s}[k - k_0] = \hat{s}[k - k_0]/\hat{s}[k - k_0 - 1]$).
Fig. 3 shows the bit error rate (BER) vs. $10\log_{10}(E_b/N_0)$ ($E_b = E_S/4$) for 16DAPSK ($\Delta R = 2.0$) transmitted over a channel with impulse response $h_0 = 0.304$, $h_1 = 0.903$, $h_2 = 0.304$. $L_c = 7$ and $k_0 = 4$ are adopted for NMIE and ZF equalization. As N increases the power efficiency of the noncoherent scheme improves. The performance of coherent ZF equalization is approached for $N \gg 1$. A comparison with Fig. 2 of [9] valid for noncoherent linear MMSE equalization shows that for the considered channel NMIE yields approximately the same performance as the MMSE approach.

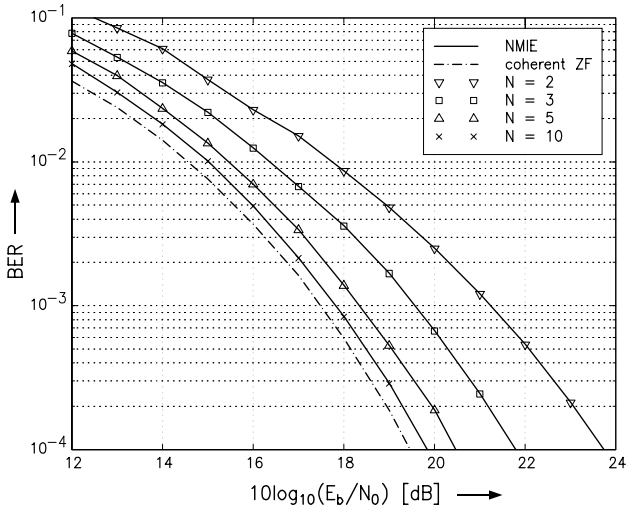

Figure 3: BER vs. $10\log_{10}(E_b/N_0)$ for 16DAPSK with NMIE. For comparison the BER for a coherent linear ZF equalizer is also shown.

So far, zero frequency offset has been assumed. However, practical receivers often have to cope with carrier phase variations. Therefore, Fig. 4 shows BER vs. normalized frequency offset ΔfT (T is the symbol duration) for QDPSK. The same channel as for Fig. 3 is used and $10\log_{10}(E_b/N_0) = 12$ dB, $L_c = 7$, and $k_0 = 4$ are valid. It can be seen, that the sensitivity to frequency offset increases with increasing N. On the other hand, for zero frequency offset power efficiency improves for higher values of N. Hence, there is a trade–off between performance under pure AWGN conditions and robustness against frequency offset. Note that a coherent ZF or MMSE equalizer degrades severely (BER = 0.5) even for very low frequency offsets ($\Delta fT < 0.0001$) since the conventional

LMS algorithm fails to follow the phase changes, i.e., in this case, an additional frequency synchronization unit is necessary. The modified LMS algorithm applied for NMIE, however, does not have to track the frequency offset since a noncoherent equalizer is applied.

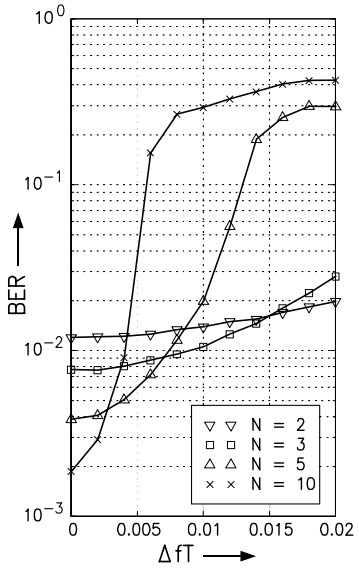

Figure 4: BER vs. ΔfT for QDPSK with NMIE.

6. Conclusions

In this paper, a novel noncoherent equalizer is presented and analyzed. It consists of the combination of a linear equalizer and a DF–DD. The proposed linear equalizer minimizes the variance of ISI in the equalizer output signal and the DF–DD removes the dependence of the decision variable on the channel phase. The optimum equalizer coefficients may be calculated from an eigenvalue problem which is obtained from a constrained optimization task.

It is shown that for infinite–length equalizers, the resulting equalization scheme is equivalent to a ZF equalizer. For an efficient adaptation of the equalizer coefficients a novel modified LMS algorithm is proposed. The convergence speed of this algorithm is comparable to that of the conventional (coherent) LMS algorithm. Simulation results demonstrate the good performance of the proposed equalization scheme and its robustness against frequency offset.

Appendix

In this appendix, x_μ (cf. (11)), $0 \leq \mu \leq L_c + L_h - 2$, $\mu \neq k_0$, and γ (cf. (12)) are calculated for some special cases:

A. $N \to \infty$

For $N \to \infty$, (11) and (12) yield

$$x_\mu = 1, \ \forall \mu, \tag{36}$$

and

$$\gamma = 1, \tag{37}$$

respectively. Note that these results are valid for arbitrary MDAPSK modulation formats.

B. MDPSK

Since $|s[k]| = 1, \forall k$, holds for MDPSK,

$$x_\mu = 1 + \frac{1}{N-1} = \frac{N}{N-1}, \ \forall \mu, \tag{38}$$

$$\gamma = 1 + \frac{1}{N-1} = \frac{N}{N-1}, \tag{39}$$

is obtained.

C. 16DAPSK

For 16DAPSK, γ can be calculated to

$$\gamma = 1 + \frac{1}{2^{N-1}} \sum_{\nu=0}^{N-1} \binom{N-1}{\nu} \frac{1}{(N-1-\nu)R_2^2 + \nu R_1^2}. \tag{40}$$

References

[1] R. W. Lucky, J. Salz, and E. J. Jr. Weldon. *Principles of Data Communication*. McGraw–Hill, New York, 1968.

[2] J.G. Proakis. *Digital Communications*. McGraw–Hill, New York, Third Edition, 1995.

[3] P. Sehier and G. Kawas Kaleh. Adaptive equaliser for differentially coherent receiver. *IEE Proceedings-I*, 137:9–12, February 1990.

[4] R. Schober, W. H. Gerstacker, and J. B. Huber. Linear Equalization Combined With Noncoherent Detection of MDPSK Signals. *To be published in IEEE Trans. on Commun.*, 2000.

[5] A. Masoomzadeh-Fard and S. Pasupathy. Nonlinear Equalization of Multipath Fading Channels with Noncoherent Demodulation. *IEEE Journal on Selected Areas in Communications*, SAC-14:512–520, April 1996.

[6] R. Schober and W. H. Gerstacker. Adaptive Noncoherent DFE for MDPSK Signals Transmitted Over ISI Channels. *To be published in IEEE Trans. on Commun.*, 2000.

[7] F. Adachi and M. Sawahashi. Decision Feedback Differential Detection of Differentially Encoded 16APSK Signals. *IEEE Trans. on Commun.*, COM-44:416–418, August 1996.

[8] R.-Y. Wei and M.-C. Lin. Modified decision feedback differential detection for differentially encoded 16 APSK signals. *Electronics Letters*, 34(4):336–337, 1998.

[9] R. Schober and W. H. Gerstacker. Noncoherent Adaptive Linear MMSE Equalization for 16DAPSK Signals. *IEE Electronics Letters*, 35(23):2006–2008, November 1999.

[10] R. Schober, W. H. Gerstacker, and J. B. Huber. Adaptive Noncoherent Linear Minimum ISI Equalization for MDPSK and MDAPSK Signals. *Submitted to IEEE Trans. on Signal Processing*, June 1999.

[11] S. Haykin. *Adaptive Filter Theory*. Prentice-Hall, Upper Saddle River, New Jersey, Third Edition, 1996.